



Clumped isotope temperature and salinity constrains for the Maastrichtian Chalk Sea based on planktonic and benthic foraminifera from Poland

Marion Peral^{1,2}, Marta Marchegiano^{1,3}, Weronika Wierny⁴, Inigo A. Müller¹, Johan Vellekoop^{5,6}, Zofia
5 Dubicka⁴, Maciej J. Bojanowski⁷, Steven Goderis¹, Philippe. Claeys¹

¹Archaeology, Environmental Changes & Geo-Chemistry, Vrije Universiteit Brussel, Brussels, 1070 Belgium

²now at: Univ. Bordeaux, CNRS, Bordeaux INP, EPOC, UMR 5805, Pessac, 33600 France

³now at: Departamento de Estratigrafía y Paleontología, Universidad de Granada

⁴University of Warsaw, Faculty of Geology, ul. Żwirki i Wigury 93, 02-089 Warszawa, Poland;

10 ⁵Biogeology & Paleoclimatology Research Group, KU Leuven, Leuven, Belgium

⁶Operational Directorate Earth and History of Life, Institute of Natural Sciences, Brussels, Belgium

⁷Institute of Geological Sciences, Polish Academy of Sciences, Warsaw, Poland

Correspondence to: Marion Peral (marion.peral@u-bordeaux.fr)

Abstract. The Maastrichtian (~72–66 Ma), the final stage of the Cretaceous, experienced long-term cooling with high
15 atmospheric CO₂ and weak latitudinal temperature gradients. Tectonic movements and variations in climate lead to sea-level changes and dynamic ocean conditions. This background probably affected the seawater circulation regime of the shallow epeiric Chalk Sea that covered a large portion of the Northern European continent. The connections to the evolving Northern Atlantic, the Arctic Basin and the tropical Thetis Ocean in the South and their impact on the seawater circulation and stratification in the open Chalk Sea is still not well understood. This study applies carbonate clumped-isotope thermometry
20 (Δ_{47}) to well preserved planktonic and benthic foraminifera from the Polanówka UW-1 core (Poland) to reconstruct the local surface and bottom water conditions prevailing during the Maastrichtian in the Chalk Sea.

The results from planktonic foraminifera reveal dynamic surface water conditions of alternating warmer and more saline with colder and less saline surface waters compared to stable, warm, and saline bottom waters from the benthic foraminifera. Comparisons with previous studies indicate the new planktonic Δ_{47} -SST reconstructions align more with oxygen isotope-
25 based SST than the SST based on organic proxies such as TEX₈₆-SST, with differences attributed to calibration, seasonality, and habitat depth. These findings suggest a stratified water column where the surface water is influenced by sporadic water entrainment with strong depleted $\delta^{18}\text{O}$ that could be associated to freshwater runoff. The observed more stable and warm bottom water conditions and the range of $\delta^{18}\text{O}$ may be associated with 2 scenarios: (1) a warm, saline bottom water periodically influenced by incursions of colder and fresher North Atlantic waters, or (2) bottom water conditions influenced
30 by increased water input from the Tethys during periods of sea-level rise. Our reconstructions on the central European Chalk Sea conditions provide new insights into the thermal structure and water circulation in the Chalk Sea during the Mid-Maastrichtian Event and highlight the need for further research to refine the understanding of hydrology dynamics during this mild greenhouse climate interval.



1 Introduction

35 The Maastrichtian (~72–66 Ma) marks the end of the Cretaceous and represents a pivotal interval in Earth's climatic history as it is seen as mild greenhouse interval. It is characterized by a long-term cooling trend associated with atmospheric CO₂ levels probably slightly higher than the modern ones, exceeding 600–1000 ppm (e.g., Royer et al., 2014; Foster et al., 2017; Steinhorsdottir et al., 2025), and an eventually weaker latitudinal temperature gradients (e.g., Huber et al., 2002; Friedrich et al., 2012). Superimposed on this long-term cooling, several episodes of climate cooling and warming during the
40 Maastrichtian, correlated with eustatic sea-level changes, indicating climate instability and enhanced ocean dynamics (e.g., Barrera and Savin, 1999; Isaza-Londoño, 2006). These short-term sea-level fluctuations have been attributed to medium-sized ice sheets in Antarctica during the early Maastrichtian (Miller et al., 1999), the aquifer-eustasia mechanism (Sames et al., 2020), or tectonic processes such as basin geometry changes and the opening of the Atlantic Ocean (Frank and Arthur, 1999; Friedrich et al., 2009; Jung et al., 2013). During this time, an extensive shallow marine basin, known as the Chalk Sea,
45 covered the northern and central part of the European continent. This epeiric sea, semi-enclosed with connections to the North Atlantic, Arctic Basin, and subtropical Tethys (Markwick and Valdes, 2004), played a crucial role in shaping regional oceanographic dynamics. Understanding the thermal structure and seawater circulation dynamics of the Chalk Sea is essential for reconstructing regional climate and the prevailing biogeochemical processes during the Late Cretaceous. It also provides insight into the mechanisms driving long-term greenhouse climates. Consequently, there is an urgent need to better
50 constrain the seawater properties of the Chalk Sea.

Earlier studies on seawater temperature variations in this region primarily relied on the $\delta^{18}\text{O}$ of biogenic carbonates (e.g., Thibault et al., 2016). However, the $\delta^{18}\text{O}$ of carbonates is also influenced by the $\delta^{18}\text{O}$ of seawater and is therefore not solely temperature dependent. The Maastrichtian is commonly considered ice-free but some studies suggest the possibility of polar ice sheets during this time (e.g., Miller et al., 1999; Thibault et al., 2016). Additionally, variations in atmospheric
55 precipitation or terrestrial freshwater input from rivers may affect seawater $\delta^{18}\text{O}$ further complicating paleotemperature interpretations. As an alternative, organic temperature proxies such as TEX₈₆ have been extensively used (e.g., Huber et al., 2002; O'Brien et al., 2017). However, TEX₈₆ provides temperature reconstructions of sea surface or subsurface (van der Weijst et al., 2022) leaving bottom water conditions and the interactions between surface and deep waters undocumented. Clumped-isotope thermometry offers an interesting alternative, as it applies to both planktonic and benthic foraminifera,
60 allowing for the reconstruction and comparison of surface and bottom water properties.

Over the past decade, clumped-isotope thermometry applied to fossilized shells (e.g., Meyer et al., 2018; 2019; Price et al., 2020; De Winter et al., 2021; O'Hora et al., 2022; Marchegiano and John, 2022; Marchegiano et al., 2024) and especially to foraminiferal shells (e.g., Rodriguez-Sanz et al., 2017; Modestou et al., 2020; Peral et al., 2020, 2022; Meinicke et al., 2020; 2021; Agterhuis et al., 2022; Meckler et al., 2022; Van der Ploeg et al., 2023), has been used increasingly to reconstruct
65 seawater temperatures. Carbonate clumped isotope thermometry (Δ_{47} hereafter) is based on the quantification of subtle statistical anomalies in the abundance of doubly substituted carbonate isotopologues ($^{13}\text{C}^{18}\text{O}^{16}\text{O}^{16}\text{O}_2$, Eiler, 2007). When



relative isotopologue abundances are governed by thermodynamic equilibrium relationship, ^{13}C - ^{18}O bonds are slightly more abundant than for a purely random distribution of isotopes, and this effect increases as equilibration temperature decreases (Schauble et al., 2006; Ghosh et al., 2006). Another great advantage of this paleothermometer lies in its independence of the $\delta^{18}\text{O}$ of water in which the calcification occurred (Schauble et al., 2006). Nevertheless, for existing Maastrichtian Δ_{47} seawater temperature data from the European Chalk Sea, North Atlantic Ocean and Tethys Ocean, the existing Maastrichtian Δ_{47} seawater temperature estimations are based on old standardization of the results (e.g. Dennis et al., 2013; Meyer et al., 2018; 2019; Tagliavento et al., 2019; O'Hora et al., 2022). This makes their comparison difficult. In addition, these records are mostly near coastal records being more influenced by local seasonal evaporation/precipitation processes. Maastrichtian clumped isotope temperature estimates on foraminifera of more open marine environments do not exist to our best knowledge. Furthermore, well-preserved fossils from deeper environments are rare, complicating the use of carbonate clumped-isotope thermometry for the Maastrichtian.

This study provides, for the first time, a deep glimpse on the variability of both surface and bottom seawater temperatures in a distal setting in the European Chalk Sea for the Maastrichtian. The Δ_{47} thermometry is applied to exceptionally well-preserved foraminifera, extracted from the Polanówka UW-1 core (Poland_ representing a non-coastal environment, deposited at mesopelagic water depths (Dubicka et al., 2024). The foraminifera include both benthic and shallow-dwelling planktonic species, allowing for a distinction between surface- and deep-water masses. The surface- and bottom-derived clumped isotope temperatures allowed to estimate the past water oxygen isotopic composition of the seawater. To better constrain the surface and deep current circulation, the Δ_{47} thermometry results are compared to the already published bulk isotopic curves and ϵNd from Dubicka et al. (2024).

2 Material and methods

The 91 m deep Polanówka UW-1 core is situated in eastern Poland (Fig. 1) and belongs to the Middle Vistula River valley composite section, an upper Cretaceous succession of the Polish Basin (Walaszczyk, 2012). The core records complete and continuous Maastrichtian strata, rich of well-preserved foraminifera as confirmed by Scanning Electron Microscope (SEM) images and elemental composition of their shells (Dubicka et al., 2024). The SEM pictures from Dubicka et al. (2024) are also presented in figure 2.

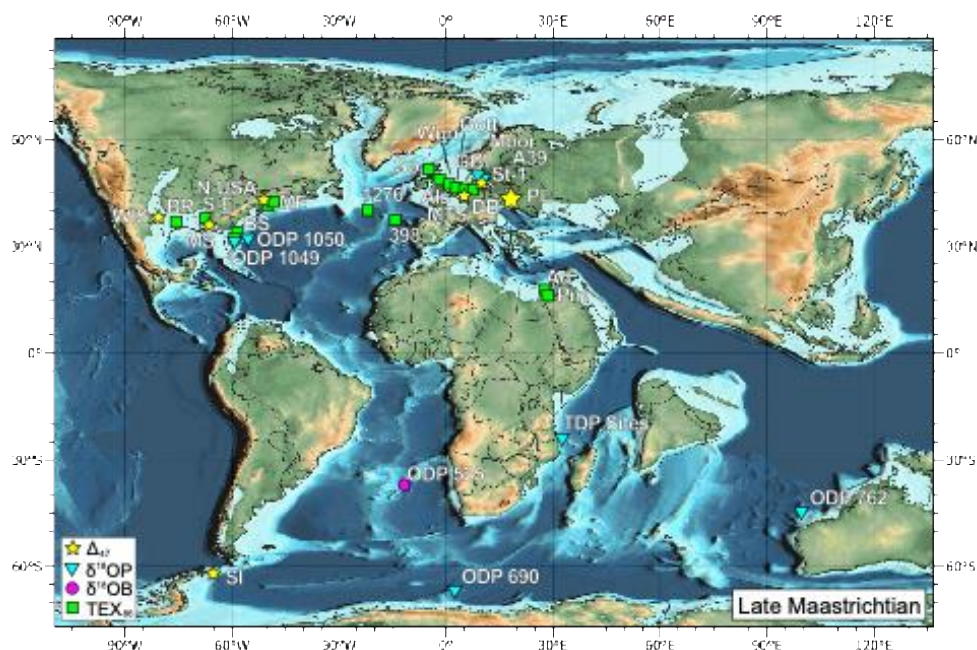
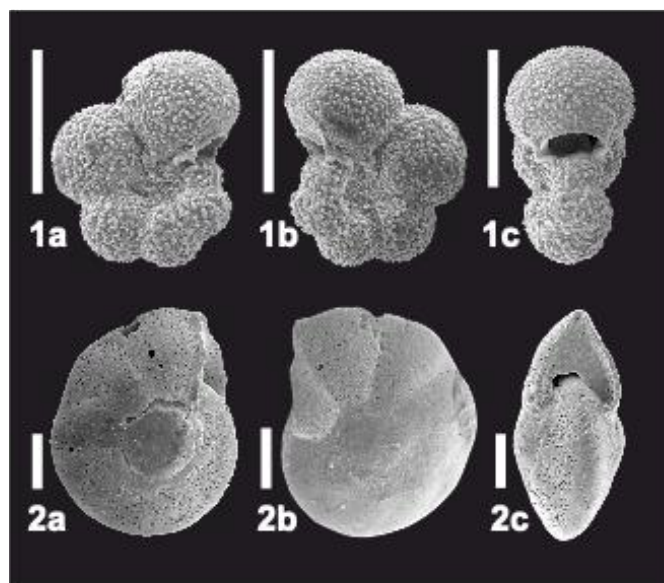


Figure 1: Paleogeographic map during the late Maastrichtian (from Scotese, 2013). PL – Polanówka UW-1; St-1 – Stevns-1; BR – Brazos River; S-E – Shuqualak-Evans; MS – Mississippi; MF – Meirs Farm; Ad – Aderet borehole 1; Pm – PAMA
95 Quarry; SI – Seymour Island; GB1 – Saxony Basin; Sp – Speeton; Als – Alstätte; Wun – Wunstorf core; Moor – Moorberg; WIS – Western Interior Seaway; DB – Danish Basin; MTS – Maastrichtian Type Section; TDP – Tanzania Drilling Project; ODP – Ocean Drilling Program. P – planktonic, B – benthic. The symbols vary depending on the thermometers. Clumped isotope sites (star symbols) can be found in Dennis et al. (2013); Petersen et al. (2016); Meyer et al. (2018); Tagliavento et al. (2019); O’Hora et al. (2022). TEX₈₆ data (square symbols) and δ¹⁸O on planktonic foraminifera (triangle symbols) are
100 available in Thibault et al. (2016) and O’Brien et al. (2017) and references therein for low to mid latitude sites. The δ¹⁸O on benthic foraminifera (circle symbol) are available in Li and Keller, 1998a,b. Our site (Polanówka UW-1) is highlighted by the larger star.



105 **Figure 2:** SEM pictures of *Planohedbergella prariehilensis* (1) and *Cibicidoides voltzianus* (2) showing a good preservation
of the shells, from Dubicka et al. (2024). Scale bars correspond to 200 μm .

Clumped isotope analysis is carried out for five samples of planktonic (*Planohedbergella prariehilensis*) and five samples of
benthic (*Cibicidoides voltzianus*) foraminiferal species coming from the same stratigraphic layers. The Δ_{47} values are
measured in the Archeology, Environmental Changes & Geo-Chemistry (AMGC) laboratory of the VUB, using a Nu
110 Instruments Perspective-IS stable isotope ratio mass spectrometer (SIRMS), in conjunction with a Nu-Carb carbonate sample
preparation system, as described in detail in De Vleeschouwer et al. (2022). A total of 393 measurements are carried out,
including 280 measurements of carbonate standards (Meckler et al., 2014; Bernasconi et al., 2018, 2021). All the samples are
replicated between 6 and 16 times (500 μg sample material per replicate). Analyses and results are monitored in the lab using
115 the Easotope software (John and Bowen, 2016). The carbonate standard ETH-4 is systematically measured and compared to
InterCarb values (Bernasconi et al., 2021) to ensure the measurements quality control. The raw measured Δ_{47} values are
processed using the IUPAC Brand's isotopic parameters (Brand et al., 2010; Daëron et al., 2016; Petersen et al., 2019) and
convert to the I-CDES90 scale, using the most recent values for the ETH-1, ETH-2, and ETH-3 carbonate reference
materials (Bernasconi et al., 2021) within the ClumpyCrunch software (Daëron et al., 2016; Daëron, 2021). The average Δ_{47}
120 values of each sample are converted into temperatures using the recalculated foraminiferal calibration from Daëron and Gray
(2023) which includes the data of Peral et al. (2018) and Meinicke et al. (2020). Both analytical and calibration uncertainties
are propagated to calculate the final uncertainties on temperatures.

The $\delta^{18}\text{O}$ of seawater ($\delta^{18}\text{O}_{\text{sw}}$) is calculated by combining the Δ_{47} -temperatures and the $\delta^{18}\text{O}$ of the foraminifera using the
temperature relation of Kim and O'Neil (1997). The bulk isotope measurements on planktonic (*Planohedbergella*



125 prariehilensis) and benthic (*Cibicoides voltzianus*) foraminifera, as well as the ϵNd obtained from powdered bulk carbonate samples are displayed in Dubicka et al. (2024).

3 Results

The clumped isotope-derived temperatures ($\Delta_{47}\text{-T}$) from planktonic foraminifera vary between 14.2°C ($\pm 2.4^\circ\text{C}$ 1SE) and 23.5°C ($\pm 3.5^\circ\text{C}$ 1SE), while the clumped isotope-derived temperatures from benthic foraminifera vary between 16.2°C ($\pm 1.6^\circ\text{C}$ 1SE) and 21.9°C ($\pm 1.8^\circ\text{C}$ 1SE; Table 1). Surprisingly, at most stratigraphic layers (at 86, 75 and 46 m depth), the $\Delta_{47}\text{-T}$ values are lower for planktonic (representing surface seawater) than for benthic foraminifera (representing bottom seawater) (Table 1). Layers with the expected warmer planktonic and colder benthic foraminifera Δ_{47} temperatures alternate with those with colder planktonic and warmer benthic Δ_{47} temperatures (Table 1). Furthermore, similar variations are observed on the $\delta^{18}\text{O}$ of seawater reconstructed from Δ_{47} and $\delta^{18}\text{O}$ of the foraminifera, with surface seawater values $\delta^{18}\text{O}_{\text{s-sw}}$ (calculated for planktonic foraminifera) between -1.0‰ ($\pm 0.4\text{‰}$ 1SE) and -3.1‰ ($\pm 0.3\text{‰}$ 1SE), and bottom seawater values $\delta^{18}\text{O}_{\text{b-sw}}$ (calculated for benthic foraminifera) between -0.8‰ ($\pm 0.2\text{‰}$ 1SE) and -1.9‰ ($\pm 0.2\text{‰}$ 1SE). The relatively enriched $\delta^{18}\text{O}_{\text{s-sw}}$ is observed when the planktonic-SST are warmer than the benthic-T, whereas the enriched $\delta^{18}\text{O}_{\text{b-sw}}$ occurs when the planktonic-SST are colder than the benthic-T (Table 1).

Dubicka et al. (2024) presented the foraminiferal stable isotope data from the same interval of the core. The $\delta^{18}\text{O}$ of planktonic ($\delta^{18}\text{O}_{\text{s}}$) and $\delta^{18}\text{O}$ of benthic foraminifera ($\delta^{18}\text{O}_{\text{b}}$) have distinct signals and vary from -0.8‰ to -1.3‰ and from -0.3‰ to -0.9‰ , respectively (Dubicka et al., 2024), with the lowest difference between $\delta^{18}\text{O}_{\text{s}}$ and $\delta^{18}\text{O}_{\text{b}}$ (0.2‰) around 65 m. The $\delta^{18}\text{O}_{\text{s}}$ and $\delta^{18}\text{O}_{\text{b}}$ obtained simultaneously with Δ_{47} , agree with Dubicka et al. (2024) data, supporting the reliability of the Δ_{47} analyses. In addition, the quality check standard (ETH 4) is good, with a value of 0.4465‰ ($\pm 0.0077\text{‰}$) – accepted values from Bernasconi et al. (2021) = 0.4505‰ ($\pm 0.0035\text{‰}$).

145

Table 1: Summary of the clumped isotope data, derived temperatures and estimated seawater $\delta^{18}\text{O}$ on benthic (B) and planktonic (P) with associated uncertainties at 1 sigma and number of replicates (of 500 μm powdered foraminifera).

Sample names	Depth	N° replicates	Δ_{47}	SE	T	SE	$\delta^{18}\text{O}_{\text{sw}}$	SE
B1	86	13	0.6099	0.0099	19.7	1.9	-1.2	0.2
B2	79	16	0.6204	0.0092	16.2	1.6	-1.9	0.2
B3	75	16	0.604	0.009	21.8	1.7	-0.8	0.2
B4	65	15	0.6036	0.0094	21.9	1.8	-1.0	0.2
B5	46	14	0.6111	0.0098	19.3	1.9	-1.5	0.2
P1	86	9	0.6263	0.0117	14.2	2.4	-3.1	0.3
P2	79	7	0.6019	0.0129	22.5	3.0	-1.2	0.3
P3	75	8	0.6217	0.0122	15.7	2.6	-2.6	0.3



P4	65	6	0.599	0.0142	23.5	3.5	-1.0	0.4
P5	46	8	0.6244	0.0123	14.8	2.6	-2.8	0.3

https://drive.google.com/file/d/1osvOM0sq86HgPkaPxEMCoTBkUw9fnTSa/view?usp=drive_link

150 4 Discussion

4.1 Are temperatures affected by species growth preferences? 1.1 Subsection

The planktonic SST and $\delta^{18}\text{O}_{\text{s-sw}}$ show higher variability of the surface water than the more constant bottom-T and $\delta^{18}\text{O}_{\text{b-sw}}$ derived from benthic foraminifera (inside the uncertainty ranges; Fig. 3). The maximum variation observed in SST and $\delta^{18}\text{O}_{\text{s-sw}}$ is of 9.3 °C and 2.1 ‰ respectively, while at the bottom, the variation is 5.7 °C and 1.1 ‰ (Table 1 and Fig. 3). These differences in variability highlight the more dynamic nature of surface water conditions, in contrast to the relative stability of bottom water conditions. Modern studies on seawater properties in the Mediterranean Sea and the shallower Baltic Sea show large seasonal temperature variations at the surface, in a similar range or larger to that obtained from our Δ_{47} -SST (e.g., Bradtke et al., 2010; Sakalli, 2017; WOA data from Locarini et al., 2018). These temperature fluctuations are more closely linked to atmospheric seasonal variations that are also expected to have been operating in the past. On the other hand, conditions at the seafloor remain more stable (WOA data from Locarini et al., 2018). The species composition and abundance of planktonic foraminifera are driven by food and nutrient availability, as well as changes in water circulation, strictly related to seasonal changes (see e.g., Kimoto, 2015). Also, as the growth season of planktonic foraminifera can be affected by seasonality, the larger variations in the record could potentially reflect slight changes in their growth season. Whereas benthic species grow more slowly over a longer time interval. Therefore, potential seasonality of living preferences between the planktonic and the benthic foraminifera may also play a role in this difference in variability between surface and bottom temperatures.

Previously published sea surface temperature data for the Maastrichtian are available for lower mid-paleolatitudes (30–48°) with SST estimates ranging from 15 to 25°C for $\delta^{18}\text{O}$ thermometer and from 25 to 30 or 35°C for TEX_{86} thermometer (O'Brien et al., 2017 and references therein). The $\delta^{18}\text{O}$ -SST estimates are consistently colder than those from TEX_{86} . This difference is attributed to assumptions regarding changes in $\delta^{18}\text{O}_{\text{sw}}$ and/or potential biases in foraminiferal $\delta^{18}\text{O}$ and/or an overestimation of SST by TEX_{86} (O'Brien et al., 2017). However, the obtained Δ_{47} temperature data align more closely with $\delta^{18}\text{O}$ -SST reconstructions than with the organic-SST estimates (Fig. 3). Since the clumped isotope method is independent of $\delta^{18}\text{O}_{\text{sw}}$, explanations involving incorrect assumptions of $\delta^{18}\text{O}_{\text{sw}}$ are unlikely. Additionally, Thibault et al. (2016) calculated $\delta^{18}\text{O}$ -SST using two different $\delta^{18}\text{O}_{\text{sw}}$ values corresponding to a world with and without ice sheets. For the Stevns-1 site (Denmark), located slightly north of the present study area, the difference between the corrections with and without ice sheets results in a shift of ~2.5°C (13.5 to 17.5°C with $\delta^{18}\text{O}_{\text{sw}}$ at -1‰ [ice-free] and 16 to 20°C with $\delta^{18}\text{O}_{\text{sw}}$ at -0.5‰ [with ice sheets]; Thibault et al., 2016). This provides further confirmation that the misestimation of $\delta^{18}\text{O}_{\text{sw}}$ cannot account for the



observed difference. The observed misfit may be rather due to variations in the living depth and/or seasonality between the archaea producing the membrane lipids on which TEX_{86} is based and the planktonic foraminifera. It is interesting to note that the only other available Δ_{47} -SST available are similar to the TEX_{86} -SST (24 to 30°C; Tagliavento et al., 2019), however, as the authors mention in their study are probably biased to summer temperatures as they are based on coccoliths with shorter growth seasons. Assuming correct absolute SST on the coccoliths, the differences with the present study foraminiferal Δ_{47} -SST adds another argument for a difference in living depth and/or seasonality between planktonic foraminifera and coccoliths.

Previously published bottom water temperature data for the Maastrichtian are available, primarily based on Δ_{47} measurements of coastal benthic species. The Δ_{47} -derived temperatures from USA records range between 10 and 15°C (Meyer et al., 2018), which are colder than the results presented here. However, direct comparison remains challenging because Meyer et al. (2018) used a different standardization methodology. In contrast, Δ_{47} measurements on bivalves from the Maastricht region (O’Hora et al., 2022) are based on similar methodology, allowing the comparison. The data from the late Maastrichtian of the type-Maastrichtian yield an average temperature of 22°C ($\pm 3^\circ\text{C}$, 1SE), which is in the range of our Δ_{47} -based temperatures in our study, and a $\delta^{18}\text{O}_{\text{sw}}$ of -0.5‰ in average, which is higher than the present reconstructions (O’Hora et al., 2022) (Fig. 3). This difference is likely due to the Maastricht region being situated at a shallower depth (several tens of meters maximum; Hart et al., 2016), compared to the Polanówka UW-1 core, and influenced by local/costal variations. Although the mid latitude Δ_{47} studies on larger benthic calcifying organisms come with a large temperature range due to the near coastal settings (Meyer et al., 2018; O’Hora et al., 2022), they are in the same range as the obtained surface temperatures in our study considering the existing spatial temperature heterogeneities also seen in modern SST data (Judd et al., 2020). Bottom water temperatures derived from $\delta^{18}\text{O}$ measurements are also available, but they were collected at different paleolatitude ranges and in opposite hemispheres, making meaningful comparisons challenging (e.g., Li and Keller, 1998a,b).

In some stratigraphic levels (at 86, 75 and 46 m depth), surface waters at Polanówka are observed to be colder and more ^{18}O -depleted than the bottom one. A similar process is observed today in the Baltic Sea (e.g., Rak and Wiczorek, 2012; Torniaainen et al., 2017), with seasonal colder and relatively ^{18}O -depleted surface water (with $\delta^{18}\text{O}_{\text{s-sw}}$ of -6 to -10 ‰) compared to the bottom water, which is characterized by warmer and relatively ^{18}O -enriched water (with $\delta^{18}\text{O}_{\text{b-sw}}$ of -5 to -6 ‰). In case of the modern Baltic Sea the source of the water mass with strongly depleted $\delta^{18}\text{O}$ originates from riverine freshwater input of the surrounding Fenno-Scandian Shield. Here, there are two potential explanations of these shifts in the water column, i.e. i) input of freshwater or ii) oceanographic changes, as detailed below.

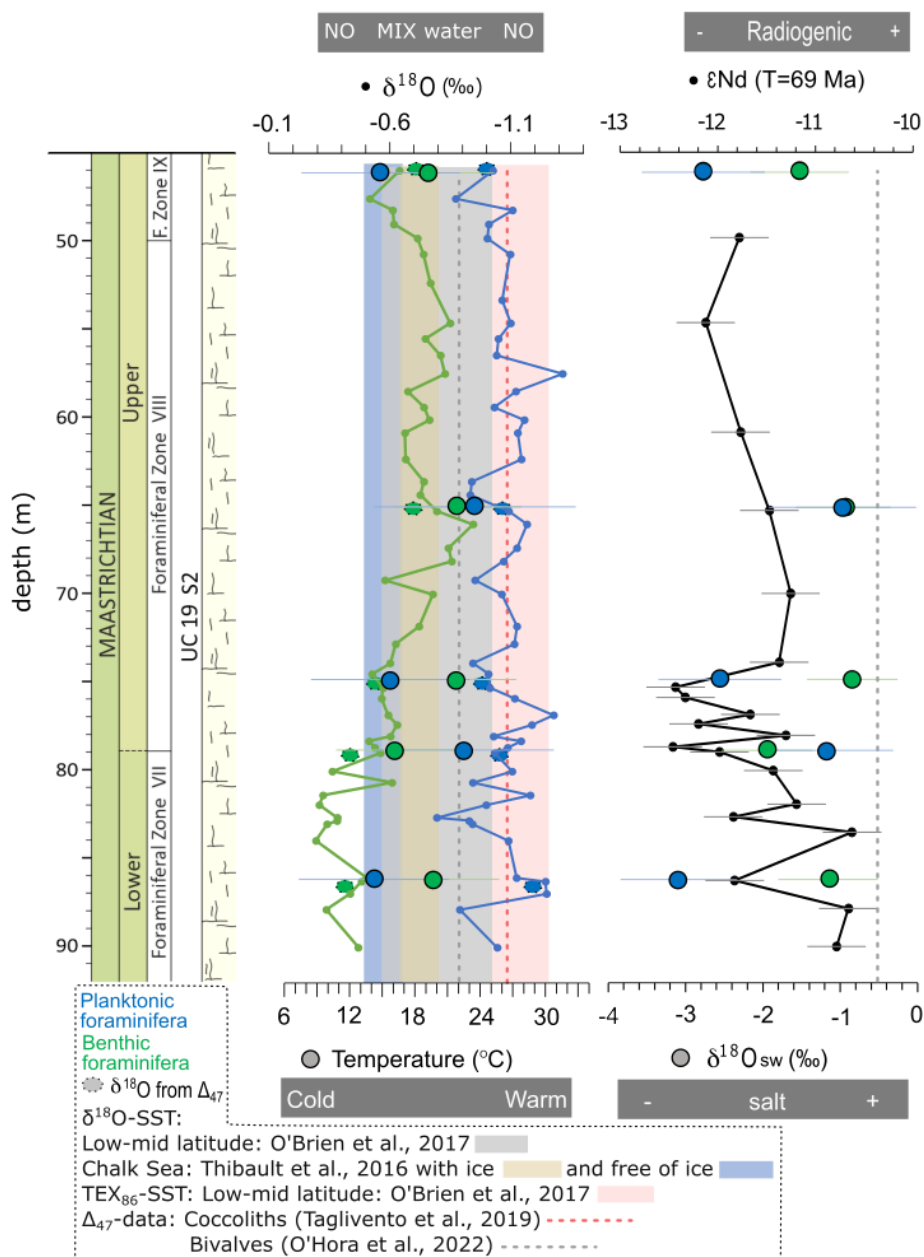


Figure 3: Clumped isotope-derived temperatures presented against depth with the $\delta^{18}\text{O}$ curves (from Dubicka et al., 2024) for benthic (green) and planktonic (blue) foraminifera. The $\delta^{18}\text{O}$ obtained simultaneously with the clumped isotope analysis are also plotted to show the good agreement. The estimated $\delta^{18}\text{O}$ seawater is represented in comparison to the ϵNd measurements (from Dubicka et al., 2024). Data are compared to the range of SST reconstructed from TEX_{86} : pink rectangle from O'Brien et al. (2017) at low-mid latitude; from $\delta^{18}\text{O}$: grey rectangle from O'Brien et al. (2017) at low-mid latitude and from Thibault et al. (2016) considering ice (yellow rectangle) and ice free (bleu rectangle); and from Δ_{47} : red dashed line



215 from Tagliavento et al. (2019) based on coccoliths. Bivalves Δ_{47} -derived temperature is also plotted, average value from
O'Hora et al. (2022) in grey dashed line. The stratigraphy and sedimentology interpretations are from Dubicka et al. (2024).
Uncertainties are at 2SE.

4.2 Fresh surface water: upwelling or runoff inputs?

The SST reconstructions show the largest variations over time and, sometimes, are even colder than the seafloor temperature
220 estimates. These cold surface water records are also associated with depleted $\delta^{18}\text{O}_{\text{sw}}$ (Fig. 3), suggesting colder and less
saline surface waters. The water column in the section examined appears well-stratified, as indicated by distinct $\delta^{18}\text{O}$ and Δ_{47}
signals between planktonic and benthic foraminiferal species, suggesting different conditions at the sea surface and the
seafloor (Fig. 3). Such conditions could be linked to upwelling events and/or freshwater input from continental runoff,
except for the samples at 65 m and 79 m depth, for which the paleotemperatures were higher at the surface than at the bottom
225 of the sea. Upwelling events, which typically result in cold and ^{18}O -depleted surface waters, would coincide with warmer
and more saline seafloor conditions in the case studied. However, this does not align with modern upwelling systems, where
the seafloor remains cold. Previous studies indicate that the Maastrichtian was characterized by a warm and wet climate
(Mishra et al., 2022). More specifically, the paleolatitude of the Maastrichtian Chalk Sea likely corresponded to a temperate
climate, with paratropical to subtropical evergreen forests and woodlands (Upchurch et al., 2007). While precipitation at
230 lower latitudes has been estimated at up to 700 mm/year at 14° (Menezes et al., 2022), comparable data for our study site's
latitude are unavailable, making precipitation-driven runoff a plausible but non testable hypothesis. Moreover, the chalk
sedimentation is characterized by very little input of terrigenous material, which is difficult to reconcile with large input of
precipitation-driven runoff.

At 65 m core depth, $\delta^{18}\text{O}_{\text{p}}$ and $\delta^{18}\text{O}_{\text{b}}$ values converge (a difference of 0.2‰; Fig. 3), and the reconstructed seawater
235 temperatures and $\delta^{18}\text{O}_{\text{sw}}$ values from planktonic and benthic sources are indistinguishable within uncertainty ranges. This
suggests a mixing of surface and deep-water masses. A sea-level change is unlikely, as benthic foraminiferal assemblages
from the Polanówka UW-1 core indicate relatively high sea levels throughout the studied section (Dubicka et al., 2024). But,
a waning of runoff during this period could be hypothesized.

The exception at 79 m records warm and ^{18}O -enriched surface waters associated with the lowest $\epsilon\text{Nd}(t)$ values (Fig. 3). Since
240 $\epsilon\text{Nd}(t)$ was measured from bulk sediments (Dubicka et al., 2024), its interpretation regarding surface or bottom water mass
or runoff changes is challenging. The progressively less radiogenic $\epsilon\text{Nd}(t)$ signature (lower $\epsilon\text{Nd}(t)$ values) could reflect
either increased continental runoff, for instance from the Fenno-Scandian Shield similar to the modern Baltic Sea, but back
then our sample site was roughly 10° further South, and/or a transient change in water circulation, introducing water masses
with less radiogenic Nd compositions. Runoff in boreal zones, driven by weathering and erosion of Precambrian shields,
245 could contribute to the less radiogenic isotopic signature of Nd in local seawater, as $\epsilon\text{Nd}(t)$ continental crust values range
between -11 to 13 (Stille et al., 1996). However, such runoff would also introduce cold water, whereas Δ_{47} data suggest
warm surface waters during the negative $\epsilon\text{Nd}(t)$ peak. Finally, the anticorrelation between reconstructed $\delta^{18}\text{O}_{\text{sw}}$ and $\epsilon\text{Nd}(t)$



values, alongside the similarity between $\delta^{18}\text{O}_{\text{b-sw}}$ and $\epsilon\text{Nd}(t)$ trends, suggests that $\epsilon\text{Nd}(t)$ values may reflect deep-water circulation changes, as interpreted by Dubicka et al. (2024). However, Pucéat et al. (2005) measured $\epsilon\text{Nd}(t)$ on fossil fish teeth from Eben-Emael in Belgium and found a more radiogenic $\epsilon\text{Nd}(t)$ values of -8.5 compared to our site. As both sites are located in the Chalk Sea, we can expect similar values, but the offset between the two is significant and can reflect the difference in the measured material or a local effect.

4.3 Change in bottom water mass circulation: Atlantic or Thetis water inputs?

The reconstructed benthic-T and $\delta^{18}\text{O}_{\text{b-sw}}$ show less variations than the surface data and are almost consistently warmer and more ^{18}O -enriched than in surface conditions (Fig. 3). Two hypotheses are proposed to explain this observation: (1) bottom water conditions in the shallow European Chalk Sea during the Maastrichtian are warm and rather saline (average temperature of 20.7 ± 1.8 °C, 1SE, and $\delta^{18}\text{O}_{\text{b-sw}}$ of -1.1 ± 0.4 ‰, 1SE), with occasional incursions of colder, less saline water, such as that at 79 m depth; or (2) the seafloor water is cold and freshened, as observed at 79 m depth (16.2 ± 1.6 °C, 1SE, and $\delta^{18}\text{O}_{\text{b-sw}}$ of -1.9 ± 0.3 ‰, 1SE), with periodic incursions of warmer, more saline water.

Hypothesis 1: A comparison with bottom water temperatures from the late Maastrichtian records of the Maastricht area (O'Hara et al., 2022), located farther north, shows similarities to the Polanówka UW-1 core records (20.7 ± 1.5 °C), except for the cold excursion at 79 m, compared to average 22 ± 3 °C for Δ_{47} on bivalves in O'Hara et al. (2022). This observation suggests that bottom water in the shallow Chalk Sea was warmer than the modern Mediterranean Sea bottom temperatures (between 13 and 14 °C from ~ 100 m depth; WOA data, Locarini et al., 2018). Also, the lighter $\delta^{18}\text{O}_{\text{sw}}$ values in the Maastrichtian type section (O'Hara et al., 2022) are in the same range as in our estimates, but come with larger variations, likely reflecting local/coastal influences due to the Maastricht section's shallower position than the Polanówka UW-1 core. The cold and ^{18}O -enriched bottom water at 79 m depth corresponds to the lowest $\epsilon\text{Nd}(t)$ values, potentially indicating a change in water supply. As discussed above, it is challenging to interpret the $\epsilon\text{Nd}(t)$ values available at our site, as the measurements were done on bulk sediment and can reflect surface, deep or a mix of water signal. When comparing the available benthic $\epsilon\text{Nd}(t)$ values in the North Atlantic (MacLeod et al., 2011 on fossil fish debris; Martin et al., 2012 on fossil fish teeth and debris) and in the Pacific or the eastern/southern Tethys (Stille et al., 1996 on peloidal grains; Soudry et al., 2006 on carbonate fluorapatite fraction; Martin et al., 2012 on fossil fish teeth and debris), systematic higher to similar values are estimated compared to the one at our site. As a result, entered water from another basin in the Maastrichtian European epicontinental basin would not reduce seawater $\epsilon\text{Nd}(t)$ at our site, and do not allow us to test hypothesis 1. However, the Tethys is considered to have been warm and saline (Alsenz et al., 2013), making it, in the regard of this hypothesis, an unlikely source for the cold, depleted bottom water recorded in the Polish Basin. Instead, colder North Atlantic deep-water temperatures during this period (Friedrich et al., 2012) better explain the coldest benthic-T values, suggesting potential North Atlantic water incursions.

Hypothesis 2: A second hypothesis is also possible. Our estimated cold bottom water temperature may be considered as the typical bottom temperature range of the Maastrichtian Chalk Sea (at 79 m depth, 16.2 ± 1.6 °C, 1SE, and $\delta^{18}\text{O}_{\text{b-sw}}$ of $-1.9 \pm$



0.3 ‰, 1SE; Table 1; Fig. 3). These cold bottom temperatures are closer to modern bottom temperatures in the Mediterranean Sea (between 13 and 14 °C from ~ 100 m depth; WOA, Locarini et al., 2018), which aligns better with the common view of the Maastrichtian as a period slightly warmer than today. Assuming that the reconstructed warm bottom temperatures align with the estimated surface water temperature range of the Tethys (Alsenz et al., 2013), this raises the possibility of exchanges with the Tethys, potentially driven by sea-level rise. Such exchanges are proposed to explain the Late Cretaceous formation of chalk, opoka, and siliceous nodules observed in the European Basin. In fact, sea-level rise, extensive volcanic activity, ocean floor spreading, and active ocean ridges would have increased the silicon (Si) concentration in seawater, influencing siliceous organism development in epicontinental basins (Racki and Cordey, 2000; Conley et al., 2017; Jurkowska et al., 2019, 2020a, 2020b). Potential Tethys-Chalk Sea exchanges (Jurkowska et al., 2019 and references therein) support this hypothesis. However, no silica enrichment is found in the Polanówka core (Dubicka et al., 2024).

With our dataset and available published data at the studied site, we cannot discriminate between these two hypotheses. Both remain valuable and additional data or models are needed to better constrain this regional circulation.

5 Conclusion

This study provides the first clumped isotope data constraining both surface and bottom condition of the central Chalk Sea during the MME. The planktonic SST and $\delta^{18}\text{O}_{\text{sw}}$ show greater variability than benthic temperatures and $\delta^{18}\text{O}_{\text{b-sw}}$, reflecting dynamic surface conditions and relatively stable seafloor environments, likely influenced by seasonality and/or depth organism growth preferences. Comparisons with previous studies suggest that $\Delta_{47}\text{-SST}$ align more closely with milder $\delta^{18}\text{O}\text{-SST}$ than $\text{TEX}_{86}\text{-SST}$ reconstructions, and differences in temperature ranges between datasets are attributed to variations in calibration methods, living depth, and seasonality.

The SST reconstructions indicate significant variations, with colder and less saline surface waters compared to seafloor temperatures, likely due to upwelling and/or freshwater runoff, though exceptions at 65 m and 79 m depths suggest distinct processes such as water mass mixing or waning of runoff.

The present findings suggest two potential scenarios for Maastrichtian benthic conditions in the European Chalk Sea: (1) a generally warmer and saltier bottom water with periodic incursions of colder, less saline water likely linked to North Atlantic influences, or (2) warm conditions shaped by exchanges with the Tethys during periods of sea-level rise, contributing to the characteristic Late Cretaceous chalk and siliceous deposits. These results underscore the need for additional reconstructions to refine existing understanding of oceanographic circulation and its broader implications during the Maastrichtian.

310 Data availability

The clumped-isotope data will be uploaded in EarthChem. <https://www.earthchem.org/>



The other data from the Polanówka UW-1 core are available in Dubicka et al. (2024).

Author contributions

MP, MM, WW, ZD, MB, SG and PC designed the study. WW prepared the samples for foraminifera extraction and picked
315 the foraminifera for the clumped isotope measurements. MP and WW prepared the samples for the isotopic measurements
and MP and MM carried out the clumped isotope measurements. MP, IM and JV performed the preliminary interpretations
of the results. WW, ZD and MB provide other sedimentary and geochemical proxies already published. All the authors
contributed to the writing process.

Competing interests

320 The authors declare that they have no conflict of interest.

Acknowledgements

Financial support

The study was funded by the National Science Centre, Poland, grant no. 2017/27/B/ST10/00687 given to Z.D. The research
of MP has been supported by the VUB (OZR opvangmandaat' number 3772) and Research Foundation – Flanders (FWO)
325 (senior postdoctoral grant 208064/1255923N LV 4508). The VUB Strategic Program, and the Research Foundation Flanders
(FWO) Hercules Program funded PC for the acquisition of the IRMS used in this study for the isotopic measurements.

References

- Agterhuis, T., Ziegler, M., de Winter, N. J., & Lourens, L. J. (2022). Warm deep-sea temperatures across Eocene Thermal
Maximum 2 from clumped isotope thermometry. *Communications Earth & Environment*, 3(1), 39.
- 330 Alsenz, H., Regnery, J., Ashkenazi-Polivoda, S., Meilijson, A., Ron-Yankovich, L., Abramovich, S., ... & Püttmann, W.
(2013). Sea surface temperature record of a Late Cretaceous tropical Southern Tethys upwelling system. *Palaeogeography,
Palaeoclimatology, Palaeoecology*, 392, 350-358.
- Barrera, E., & Savin, S. M. (1999). Evolution of late Campanian-Maastrichtian marine climates and oceans.
- Bernasconi, S. M., Müller, I. A., Bergmann, K. D., Breitenbach, S. F., Fernandez, A., Hodell, D. A., ... & Ziegler, M. (2018).
335 Reducing uncertainties in carbonate clumped isotope analysis through consistent carbonate-based standardization.
Geochemistry, Geophysics, Geosystems, 19(9), 2895-2914.
- Bernasconi, S. M., Daëron, M., Bergmann, K. D., Bonifacie, M., Meckler, A. N., Affek, H. P., ... & Ziegler, M. (2021).
InterCarb: A community effort to improve interlaboratory standardization of the carbonate clumped isotope thermometer
using carbonate standards. *Geochemistry, Geophysics, Geosystems*, 22(5), e2020GC009588.



- 340 Brand, W. A., Assonov, S. S., & Coplen, T. B. (2010). Correction for the 17O interference in δ (^{13}C) measurements when analyzing CO₂ with stable isotope mass spectrometry (IUPAC Technical Report). *Pure and Applied Chemistry*, 82(8), 1719-1733.
- Bradtke K., Herman A. & Urbański J.A. (2010) Spatial and interannual variations of seasonal sea surface temperature patterns in the Baltic Sea. *Oceanologia* 52, 345-362.
- 345 Conley, D. J., Frings, P. J., Fontorbe, G., Clymans, W., Stadmark, J., Hendry, K. R., ... & De La Rocha, C. L. (2017). Biosilicification drives a decline of dissolved Si in the oceans through geologic time. *Frontiers in Marine Science*, 4, 397.
- Daëron, M., Blamart, D., Peral, M., & Affek, H. P. (2016). Absolute isotopic abundance ratios and the accuracy of $\Delta 47$ measurements. *Chemical Geology*, 442, 83-96.
- Daëron, M. (2021). Full propagation of analytical uncertainties in $\Delta 47$ measurements. *Geochemistry, Geophysics, Geosystems*, 22(5), e2020GC009592.
- 350 Daëron, M., & Gray, W. R. (2023). Revisiting oxygen-18 and clumped isotopes in planktic and benthic foraminifera. *Paleoceanography and Paleoclimatology*, 38(10), e2023PA004660.
- Dennis, K. J., Cochran, J. K., Landman, N. H., & Schrag, D. P. (2013). The climate of the Late Cretaceous: New insights from the application of the carbonate clumped isotope thermometer to Western Interior Seaway macrofossil. *Earth and Planetary Science Letters*, 362, 51-65.
- 355 De Vleeschouwer, D., Peral, M., Marchegiano, M., Füllberg, A., Meinicke, N., Pälike, H., ... & Claeys, P. (2022). Plio-Pleistocene Perth Basin water temperatures and Leeuwin Current dynamics (Indian Ocean) derived from oxygen and clumped-isotope paleothermometry. *Climate of the Past*, 18(5), 1231-1253.
- De Winter, N. J., Müller, I. A., Kocken, I. J., Thibault, N., Ullmann, C. V., Farnsworth, A., ... & Ziegler, M. (2021). Absolute seasonal temperature estimates from clumped isotopes in bivalve shells suggest warm and variable greenhouse climate. *Communications Earth & Environment*, 2(1), 121.
- 360 Dubicka, Z., Wierny, W., Bojanowski, M. J., Rakociński, M., Walaszczyk, I., & Thibault, N. (2024). Multi-proxy record of the mid-Maastrichtian event in the European Chalk Sea: Paleooceanographic implications. *Gondwana Research*, 129, 1-22.
- Eiler, J. M. (2007). "Clumped-isotope" geochemistry—The study of naturally-occurring, multiply-substituted isotopologues. *Earth and planetary science letters*, 262(3-4), 309-327.
- 365 Frank, T. D., & Arthur, M. A. (1999). Tectonic forcings of Maastrichtian ocean-climate evolution. *Paleoceanography*, 14(2), 103-117.
- Friedrich, O., Herrle, J. O., Wilson, P. A., Cooper, M. J., Erbacher, J., & Hemleben, C. (2009). Early Maastrichtian carbon cycle perturbation and cooling event: Implications from the South Atlantic Ocean. *Paleoceanography*, 24(2).
- 370 Friedrich, O., Norris, R. D., & Erbacher, J. (2012). Evolution of middle to Late Cretaceous oceans—a 55 my record of Earth's temperature and carbon cycle. *Geology*, 40(2), 107-110.
- Foster, G. L., Royer, D. L., & Lunt, D. J. (2017). Future climate forcing potentially without precedent in the last 420 million years. *Nature communications*, 8(1), 14845.



- Ghosh, P., Adkins, J., Affek, H., Balta, B., Guo, W., Schauble, E. A., ... & Eiler, J. M. (2006). 13C–18O bonds in carbonate
375 minerals: A new kind of paleothermometer. *Geochimica et Cosmochimica Acta*, 70(6), 1439-1456.
- Hart, M. B., FitzPatrick, M. E., & Smart, C. W. (2016). The Cretaceous/Paleogene boundary: Foraminifera, sea grasses, sea
level change and sequence stratigraphy. *Palaeogeography, Palaeoclimatology, Palaeoecology*, 441, 420-429.
- Huber, B. T., Norris, R. D., & MacLeod, K. G. (2002). Deep-sea paleotemperature record of extreme warmth during the
Cretaceous. *Geology*, 30(2), 123-126.
- 380 Isaza Londoño, J. L. (2006). Centenarios de la Independencia. Special Issue of *Apuntes: Pontificia Universidad Javeriana*,
19(2), 169-316.
- John, C. M., & Bowen, D. (2016). Community software for challenging isotope analysis: First applications of ‘Easotope’ to
clumped isotopes. *Rapid Communications in Mass Spectrometry*, 30(21), 2285-2300.
- Judd E.J., Bhattacharya T., Ivany L.C. (2020) A dynamical framework for interpreting ancient sea surface temperatures.
385 *Geophysical Research Letters* 47, e2020GL089044. <https://doi.org/10.1029/2020GL089044>
- Jung, C., Voigt, S., Friedrich, O., Koch, M. C., & Frank, M. (2013). Campanian-Maastrichtian ocean circulation in the
tropical Pacific. *Paleoceanography*, 28(3), 562-573.
- Jurkowska, A., Świerczewska-Gładysz, E., Bąk, M., & Kowalik, S. (2019). The role of biogenic silica in the formation of
Upper Cretaceous pelagic carbonates and its palaeoecological implications. *Cretaceous Research*, 93, 170-187.
- 390 Jurkowska, A., & Świerczewska-Gładysz, E. (2020a). Evolution of Late Cretaceous Si cycling reflected in the formation of
siliceous nodules (flints and cherts). *Global and Planetary Change*, 195, 103334.
- Jurkowska, A., & Świerczewska-Gładysz, E. (2020b). New model of Si balance in the Late Cretaceous epicontinental
European Basin. *Global and Planetary Change*, 186, 103108.
- Kim, S.-T., O'Neil, J.R. (1997). Equilibrium and nonequilibrium oxygen isotope effects in synthetic carbonates. *Geochimica
395 et Cosmochimica Acta* 61, 3461–3475.
- Kimato, K. (2015). Planktic Foraminifera, in S. Ohtsuka et al. (eds.), *Marine Protists: Diversity and Dynamics*. Springer,
Tokyo, 129-178.
- Li, L., & Keller, G. (1998a). Abrupt deep-sea warming at the end of the Cretaceous. *Geology*, 26(11), 995-998.
- Li, L., & Keller, G. (1998b). Maastrichtian climate, productivity and faunal turnovers in planktic foraminifera in South
400 Atlantic DSDP sites 525A and 21. *Marine Micropaleontology*, 33(1-2), 55-86.
- Locarnini, M. M., Mishonov, A. V., Baranova, O. K., Boyer, T. P., Zweng, M. M., Garcia, H. E., ... & Smolyar, I. (2018).
World ocean atlas 2018, volume 1: Temperature.
- MacLeod, K. G., Isaza Londoño, C., Martin, E. E., Jiménez Berrocoso, Á., & Basak, C. (2011). Changes in North Atlantic
circulation at the end of the Cretaceous greenhouse interval. *Nature Geoscience*, 4(11), 779-782.
- 405 Markwick, P. J., & Valdes, P. J. (2004). Palaeo-digital elevation models for use as boundary conditions in coupled ocean–
atmosphere GCM experiments: a Maastrichtian (late Cretaceous) example. *Palaeogeography, Palaeoclimatology,
Palaeoecology*, 213(1-2), 37-63.



- Marchegiano, M., & John, C. M. (2022). Disentangling the impact of global and regional climate changes during the middle Eocene in the Hampshire Basin: new insights from carbonate clumped isotopes and ostracod assemblages. *Paleoceanography and Paleoclimatology*, 37(2), e2021PA004299.
- Marchegiano, M., Peral, M., Venderickx, J., Martens, K., García-Alix, A., Snoeck, C., ... & Claeys, P. (2024). The ostracod clumped-isotope thermometer: A novel tool to accurately quantify continental climate changes. *Geophysical Research Letters*, 51(4), e2023GL107426.
- Martin, E. E., MacLeod, K. G., Berrocoso, A. J., & Bourbon, E. (2012). Water mass circulation on Demerara Rise during the Late Cretaceous based on Nd isotopes. *Earth and Planetary Science Letters*, 327, 111-120.
- Meckler, A. N., Ziegler, M., Millán, M. I., Breitenbach, S. F., & Bernasconi, S. M. (2014). Long-term performance of the Kiel carbonate device with a new correction scheme for clumped isotope measurements. *Rapid Communications in Mass Spectrometry*, 28(15), 1705-1715.
- Meckler, A. N., Sexton, P. F., Piasecki, A. M., Leutert, T. J., Marquardt, J., Ziegler, M., ... & Bernasconi, S. M. (2022). Cenozoic evolution of deep ocean temperature from clumped isotope thermometry. *Science*, 377(6601), 86-90.
- Meinicke, N., Ho, S. L., Hannisdal, B., Nürnberg, D., Tripathi, A., Schiebel, R., & Meckler, A. N. (2020). A robust calibration of the clumped isotopes to temperature relationship for foraminifers. *Geochimica et Cosmochimica Acta*, 270, 160-183.
- Meinicke, N., Reimi, M. A., Ravelo, A. C., & Meckler, A. N. (2021). Coupled Mg/Ca and clumped isotope measurements indicate lack of substantial mixed layer cooling in the Western Pacific Warm Pool during the last ~ 5 million years. *Paleoceanography and Paleoclimatology*, 36(8), e2020PA004115.
- Menezes, M. N., Dal'Bó, P. F., Smith, J. J., Rodrigues, A. G., & Rodríguez-Berriguete, Á. (2022). Maastrichtian atmospheric p CO₂ and climatic reconstruction from carbonate paleosols of the Marília Formation (southeastern Brazil). *Journal of Sedimentary Research*, 92(9), 775-796.
- Meyer, K. W., Petersen, S. V., Lohmann, K. C., & Winkelstern, I. Z. (2018). Climate of the Late Cretaceous North American Gulf and Atlantic Coasts. *Cretaceous Research*, 89, 160-173.
- Meyer, K. W., Petersen, S. V., Lohmann, K. C., Blum, J. D., Washburn, S. J., Johnson, M. W., ... & Winkelstern, I. Z. (2019). Biogenic carbonate mercury and marine temperature records reveal global influence of Late Cretaceous Deccan Traps. *Nature communications*, 10(1), 5356.
- Miller, K. G., Barrera, E., Olsson, R. K., Sugarman, P. J., & Savin, S. M. (1999). Does ice drive early Maastrichtian eustasy?. *Geology*, 27(9), 783-786.
- Mishra, S., Singh, S. P., Arif, M., Singh, A. K., Srivastava, G., Ramesh, B. R., & Prasad, V. (2022). Late Maastrichtian vegetation and palaeoclimate: palynological inferences from the Deccan Volcanic Province of India. *Cretaceous Research*, 133, 105126.



- 440 Modestou, S. E., Leutert, T. J., Fernandez, A., Lear, C. H., & Meckler, A. N. (2020). Warm middle Miocene Indian Ocean bottom water temperatures: Comparison of clumped isotope and Mg/Ca-based estimates. *Paleoceanography and Palaeoclimatology*, 35(11), e2020PA003927.
- O'Brien, C. L., Robinson, S. A., Pancost, R. D., Damsté, J. S. S., Schouten, S., Lunt, D. J., ... & Wrobel, N. E. (2017). Cretaceous sea-surface temperature evolution: Constraints from TEX86 and planktonic foraminiferal oxygen isotopes. *Earth-Science Reviews*, 172, 224-247.
- 445 O'Hora, H. E., Petersen, S. V., Vellekoop, J., Jones, M. M., & Scholz, S. R. (2022). Clumped-isotope-derived climate trends leading up to the end-Cretaceous mass extinction in northwest Europe. *Climate of the Past Discussions*, 2021, 1-28.
- Peral, M., Daéron, M., Blamart, D., Bassinot, F., Dewilde, F., Smialkowski, N., ... & Waelbroeck, C. (2018). Updated calibration of the clumped isotope thermometer in planktonic and benthic foraminifera. *Geochimica et Cosmochimica Acta*, 450 239, 1-16.
- Peral, M., Blamart, D., Bassinot, F., Daéron, M., Dewilde, F., Rebaubier, H., ... & Ciaranfi, N. (2020). Changes in temperature and oxygen isotopic composition of Mediterranean water during the Mid-Pleistocene transition in the Montalbano Jonico section (southern Italy) using the clumped-isotope thermometer. *Palaeogeography, Palaeoclimatology, Palaeoecology*, 544, 109603.
- 455 Peral, M., Bassinot, F., Daéron, M., Blamart, D., Bonnin, J., Jorissen, F., ... & Gray, W. R. (2022). On the combination of the planktonic foraminiferal Mg/Ca, clumped ($\Delta 47$) and conventional ($\delta 18O$) stable isotope paleothermometers in palaeoceanographic studies. *Geochimica et Cosmochimica Acta*, 339, 22-34.
- Petersen, S. V., Defliese, W. F., Saenger, C., Daéron, M., Huntington, K. W., John, C. M., ... & Winkelstern, I. Z. (2019). Effects of improved $17O$ correction on interlaboratory agreement in clumped isotope calibrations, estimates of mineral-specific offsets, and temperature dependence of acid digestion fractionation. *Geochemistry, Geophysics, Geosystems*, 20(7), 460 3495-3519.
- Philip, J., Floquet, M., Platel, J. P., Bergerat, F., Sandulescu, M., Baraboshkin, E., ... & Lepvrier, C. (2000). Early Campanian (83–80 Ma). *Atlas Peri-Tethys, Paleogeographical Maps: CCGM/CGMW Paris, Map*, 15.
- Price, G. D., Bajnai, D., & Fiebig, J. (2020). Carbonate clumped isotope evidence for latitudinal seawater temperature 465 gradients and the oxygen isotope composition of Early Cretaceous seas. *Palaeogeography, Palaeoclimatology, Palaeoecology*, 552, 109777.
- Pucéat, E., Lécuyer, C., & Reisberg, L. (2005). Neodymium isotope evolution of NW Tethyan upper ocean waters throughout the Cretaceous. *Earth and Planetary Science Letters*, 236(3-4), 705-720.
- Rak, D., & Wiczcerek, P. (2012). Variability of temperature and salinity over the last decade in selected regions of the 470 southern Baltic Sea. *Oceanologia*, 54(3), 339-354.
- Racki, G., & Cordey, F. (2000). Radiolarian palaeoecology and radiolarites: is the present the key to the past?. *Earth-Science Reviews*, 52(1-3), 83-120.



- Rodríguez-Sanz, L., Bernasconi, S. M., Marino, G., Heslop, D., Mueller, I. A., Fernandez, A., ... & Rohling, E. J. (2017). Penultimate deglacial warming across the Mediterranean Sea revealed by clumped isotopes in foraminifera. *Scientific Reports*, 7(1), 16572.
- 475
- Royer, D. L., Donnadieu, Y., Park, J., Kowalczyk, J., & Godderis, Y. (2014). Error analysis of CO₂ and O₂ estimates from the long-term geochemical model GEOCARBSULF. *American Journal of Science*, 314(9), 1259-1283.
- Sakalli, A. (2017). Sea surface temperature change in the Mediterranean Sea under climate change: a linear model for simulation of the sea surface temperature up to 2100.
- 480
- Sames, B., Wagreich, M., Conrad, C. P., & Iqbal, S. (2020). Aquifer-eustasy as the main driver of short-term sea-level fluctuations during Cretaceous hothouse climate phases. *Geological Society, London, Special Publications*, 498(1), 9-38.
- Schauble, E. A., Ghosh, P., & Eiler, J. M. (2006). Preferential formation of ¹³C–¹⁸O bonds in carbonate minerals, estimated using first-principles lattice dynamics. *Geochimica et Cosmochimica Acta*, 70(10), 2510-2529.
- Scotese, C. R. (2013). PALEOMAP Paleo Atlas for ArcGIS. *Cretaceous, PALEOMAP Project, Evanston, I.*
- 485
- Soudry, D., Glenn, C. R., Nathan, Y., Segal, I., & VonderHaar, D. (2006). Evolution of Tethyan phosphogenesis along the northern edges of the Arabian–African shield during the Cretaceous–Eocene as deduced from temporal variations of Ca and Nd isotopes and rates of P accumulation. *Earth-Science Reviews*, 78(1-2), 27-57.
- Stille, P., Steinmann, M., & Riggs, S. R. (1996). Nd isotope evidence for the evolution of the paleocurrents in the Atlantic and Tethys Oceans during the past 180 Ma. *Earth and Planetary Science Letters*, 144(1-2), 9-19.
- 490
- Steinthorsdottir, M., Montañez, I. P., Royer, D. L., Mills, B. J., & Hönisch, B. (2025). Phanerozoic atmospheric CO₂ reconstructed with proxies and models: Current understanding and future directions. *Treatise on Geochemistry*, 467-492.
- Tagliavento, M., John, C. M., & Stemmerik, L. (2019). Tropical temperature in the Maastrichtian Danish Basin: Data from coccolith $\Delta 47$ and $\delta 18O$. *Geology*, 47(11), 1074-1078.
- Thibault, N., Harlou, R., Schovsbo, N. H., Stemmerik, L., & Surlyk, F. (2016). Late Cretaceous (late Campanian–
- 495
- Maastrichtian) sea-surface temperature record of the Boreal Chalk Sea. *Climate of the Past*, 12(2), 429-438.
- Torniainen J., Lensu A., Vuorinen P., Sonninen E., Keinänen M., Jones R.I., Patterson W.P. and Kiljunen M. (2017) Oxygen and carbon isoscapes for the Baltic Sea: Testing their applicability in fish migration studies. *Ecology and Evolution* 7, 2255-2267.
- Upchurch, G. R., Lomax, B. H., & BeerLing, D. J. (2007). Paleobotanical evidence for climatic change across the
- 500
- Cretaceous-Tertiary boundary, North America: Twenty years after Wolfe and Upchurch. *COURIER-FORSCHUNGSINSTITUT SENCKENBERG*, 258, 57.
- Van Der Ploeg, R., Cramwinckel, M. J., Kocken, I. J., Leutert, T. J., Bohaty, S. M., Fokkema, C. D., ... & Sluijs, A. (2023). North Atlantic surface ocean warming and salinization in response to middle Eocene greenhouse warming. *Science Advances*, 9(4), eabq0110.
- 505
- Walaszczyk, I. (2012). Integrated stratigraphy of the Campanian Maastrichtian boundary succession of the Middle Vistula River (central Poland) section; introduction. *Acta Geologica Polonica*, 62, 485-493 DOI: 10.2478/v10263-012-0027-6



- Van der Weijst C.M.H., van der Laan K.J., Peterse F., Reichert G.-J., Sangiorgi F., Schouten S., Veenstra T.J.T. and Sluijs A. (2022) A 15-million-year surface- and subsurface-integrated TEX86 temperature record from the eastern equatorial Atlantic. *Climate of the Past* 18, 1947-1962. <https://doi.org/10.5194/cp-18-1947-2022>
- 510 Ziegler, P. A. (1990). *Geological atlas of western and central Europe* (Vol. 52). The Hague: Shell Internationale Petroleum Maatschappij BV.